Radiocarbon, Vol 63, Nr 6, 2021, p 1591–1605 DOI:10.1017/RDC.2021.51

BOMB-PRODUCED RADIOCARBON ACROSS THE SOUTH PACIFIC GYRE—A NEW RECORD FROM AMERICAN SAMOA WITH UTILITY FOR FISHERIES SCIENCE

Allen H Andrews[1] • Nancy G Prouty[2*] • Olivia M Cheriton[2]

[1]University of Hawaii at Manoa, Department of Oceanography, 1000 Pope Road, Honolulu, HI 96822, USA
[2]U.S. Geological Survey, Pacific Coastal & Marine Science Center, 2885 Mission Street, Santa Cruz, CA 95060, USA

ABSTRACT. Coral skeletal structures can provide a robust record of nuclear bomb produced ^{14}C with valuable insight into air-sea exchange processes and water movement with applications to fisheries science. To expand these records in the South Pacific, a coral core from Tutuila Island, American Samoa was dated with density band counting covering a 59-yr period (1953–2012). Seasonal signals in elemental ratios (Sr/Ca and Ba/Ca) and stable carbon ($\delta^{13}C$) values across the coral core corroborated the well-defined annual band structure and highlighted an ocean climate shift from the 1997–1998 El Niño. The American Samoa coral ^{14}C measurements were consistent with other regional records but included some notable differences across the South Pacific Gyre (SPG) at Fiji, Rarotonga, and Easter Island that can be attributed to decadal ocean climate cycles, surface residence times and proximity to the South Equatorial Current. An analysis of the post-peak ^{14}C decline associated with each coral record indicated ^{14}C levels are beginning to merge for the SPG. This observation, coupled with otolith measurements from American Samoa, reinforces the perspective that bomb ^{14}C dating can be performed on fishes and other marine organisms of the region using the post-peak ^{14}C decline to properly inform fisheries management in the South Pacific.

KEYWORDS: chronology, coral, fish, radiocarbon, skeletal analysis.

INTRODUCTION

Coral records of bomb-produced radiocarbon (^{14}C) from atmospheric testing of thermonuclear devices are now sparsely available across the tropical and subtropical Pacific Ocean, ranging from the most northerly in the world at Kure Atoll (Hawaiian Archipelago; Dana 1971; Andrews et al. 2016c) to Easter Island (Rapa Nui, Chile; Biddulf et al. 2006) in the south, with various records across the Indo-Pacific region from the Great Barrier Reef to Japan and the Indian Ocean (e.g., Grumet et al. 2004; Mitsuguchi et al. 2016; Ramos et al. 2019, Wu et al. 2021). In general, bomb-produced ^{14}C in the 1950s entered the mixed layer of tropical and subtropical oceans through air-sea diffusion in the late 1950s (Grottoli and Eakin 2007). Observed differences among coral ^{14}C records arise from surface-water mixing with older, upwelled ^{14}C-depleted waters, coupled with variable air-sea diffusion rates due to wind forcing, ocean temperature, and differential air-sea CO_2 saturation states. These effects are manifested across the Pacific Ocean as differences in the magnitude and timing of the bomb ^{14}C peak and post-peak decline (Druffel 2002). Despite these differences, the ^{14}C rise period (~1958–1968) has proved useful as a time-specific marker in age validation studies of various marine organisms that form conserved skeletal and non-skeletal structures throughout the Pacific Ocean (Kalish 1993; Fallon et al. 2003; Darenougue et al. 2013; Andrews et al. 2015; Kubota et al. 2018).

Many of these Pacific coral ^{14}C records provide evidence of post-peak ^{14}C declines that point to a convergence among the various ^{14}C records that may be useful in other age validation studies (Andrews et al. 2016a, 2016c; Ramos et al. 2019; Wu et al. 2021). Specifically, bomb ^{14}C dating of fishes typically requires that the specimen lived through the late 1950s to mid-1960s to use the diagnostic ^{14}C rise period as a chronological reference, but some fishes may not have a long lifespan (on the order of 1–3 decades) or archived otoliths available that would provide birth years in the bomb ^{14}C rise period; however, the post-peak ^{14}C decline period provides a novel

*Corresponding author. Email: nprouty@usgs.gov

approach to determining the age of shorter-lived fishes from recent collections, such as the ulua or giant trevally (*Caranx ignobilis*) of the Hawaiian Islands that was validated with bomb ^{14}C dating to live 25 yr using this approach (Andrews 2020). Other recent investigations that are similar provided the first valid estimates of age for blue marlin (*Makaira nigricans*) to ~20 yr and Pacific bluefin tuna (*Thunnus orientalis*) to ~30 yr with birth years during the post-peak decline period in the 1980s to 2000s (Ishihara et al. 2017; Andrews et al. 2018). Hence, more comprehensive reference records that can extend the bomb-produced ^{14}C chronology in both time and space for the tropical and subtropical Pacific Ocean should be pursued as a tool for these unique and important fisheries studies.

The focus of this study was to provide a robust coral chronology of bomb-produced ^{14}C from American Samoa and describe its attributes in both oceanography and as a tool in age validation studies. Located along the northern edge of the South Pacific Gyre (SPG) and in the path of the westward flowing South Equatorial Current (SEC), this record provides a unique opportunity to compare and contrast the timing and magnitude of the bomb ^{14}C signal across the SPG. Existing coral ^{14}C chronologies from Easter Island (Biddulph et al. 2006) and Rarotonga (Guilderson et al. 2000) were used to highlight the variance and distribution of the ^{14}C signal within the SPG and its response to large scale climate variability, and potential convergence of ^{14}C values through time. The American Samoa record extends the regional bomb ^{14}C reference chronology and provides support for age-based validation studies on various marine organisms of the South Pacific to properly inform fisheries management.

MATERIAL AND METHODS

The coral core was collected from a reef off the southern side of Tutuila, American Samoa, near Matautuloa Point (14.30126ºS, 170.67758ºW) on 8 April 2012 (Figure 1). The core was extracted from the top of a *Porites* sp. colony at a depth of 10 m with a pneumatic drill and diamond bit coring device 3.8 cm in diameter. The recovered core was 70–72 cm in length, with no apparent hiatus in growth. The coral core was analyzed for calcification, density, and growth rates at the Woods Hole Oceanographic Institution's Computerized Tomography (CT) Scanning Facility (Crook et al. 2013). The core was then slabbed with a double blade wet tile saw to a thickness of 7 mm, which was analyzed for density banding in X-ray images. Density bands (high- and low-density couplet) identified from both the CT scans and X-rays were used to estimate the age of the coral core and to create a robust chronology (Figure 2). The coral cores were sub-sectioned into 95 × 25 mm pieces using a diamond blade saw, sonicated three times in DI water for 10 min, dried overnight, mounted on an X-Y sample stage, and placed in a sealed Perspex chamber (under helium atmosphere) for Laser Ablation - Inductively Coupled Plasma Mass Spectrometry (LA-ICP-MS) analysis at the Marine Analytical Lab of University of California, Santa Cruz. A Photon Machines 193 nm ArF excimer laser and a Thermo X-series II quadrupole ICP-MS was used, following previously described methods (Sinclair et al. 1998; Fallon et al. 1999), with samples bracketed by three standards (NIST 610, NIST 612, and JCP-1 [a Japanese ground coral standard]). Samples and standards were ablated with a scan speed of 40 $\mu m \cdot s^{-1}$ and a laser pulse rate of 10 Hz (1 pulse per 4 μm). The elemental ratios from parallel tracks along the major growth axis and perpendicular to growth bands were smoothed to an approximate resolution of 1 data point per 150 μm using a 20-point running median to remove outliers, followed by a 10-point running mean to reduce data

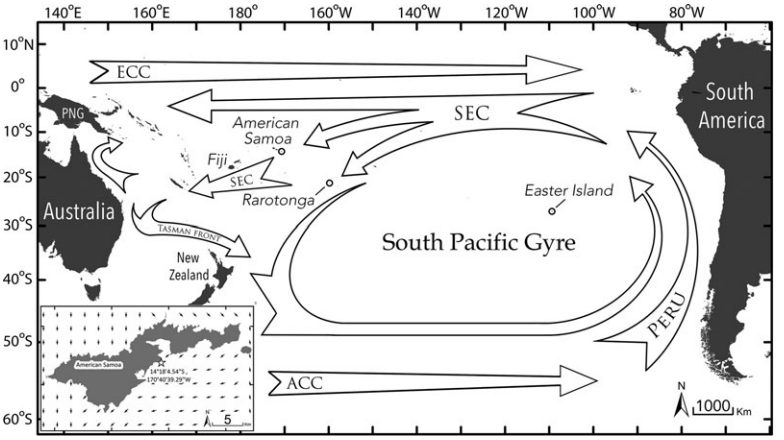

Figure 1 Map of selected locations of the tropical-subtropical South Pacific Ocean with ocean current structure for the South Pacific Gyre, a region of the South Pacific that is constrained by the Equatorial Countercurrent (ECC) and the Antarctic Circumpolar Current (ACC). The ^{14}C records from coral cores at these islands (American Samoa, Fiji, Rarotonga, and Easter Island) provide information on how the bomb-produced ^{14}C signal is affected over time and by the mixing of water sources due to climate variability (ENSO), such as changes in the strength of the South Equatorial Current (SEC) and the consequent inclusion (^{14}C-depleted) or exclusion of upwelled waters of the Peru Current to American Samoa.

volume (Jupiter et al. 2008). For visualization, data are plotted as monthly moving mean values (Supplemental Figure S1).

In preparation for ^{14}C analyses, each section of the slabbed coral core was sonicated 3 times in Milli-Q water for 5 min using a Branson 2510 sonicator. The extraction surface was faced downward during sonication to allow loose coral fragments and dust to vibrate free of the coral matrix. Slabs were thoroughly rinsed in between sonication steps and were finally air-dried in a clean, positive-pressure, laminar flow hood. A New Wave Research® micromilling machine (Elemental Scientific Lasers, LLC, Bozeman, Montana) with a 1.4 mm Brasseler® carbide cutter (H129E.11.014; Savannah, GA) was used to subsample the coral core for discrete ^{14}C measurements. Three samples were extracted across each ~1.2 cm (presumed) annual density band (yielding a sample interval of ~4 mm·yr^{-1}), which were equally spaced when possible, across the coral core (breaks in the core offset the regular interval in some places). As a result, the date of extraction was calculated based on the spacing within the density banding. Each sample consisted of a path that was 4–5 mm in length, cut 1.2 mm deep into the coral matrix, running perpendicular to the growth axis, and were not contiguous. Hence, each extraction path sampled ~12% of each year (~1.5 months) and may have missed actual high and low ^{14}C values for the coral core time series during a given year, as opposed to contiguous months-wide samples that would average out high and low values. Collection of the powdered sample was carefully performed using a fine-tipped probe, onto wax paper, and into a clean polypropylene vial (0.6 mL snap-cap centrifuge tubes) with a target mass of ~4–7 mg per sample.

In addition to the coral sample series, otoliths from juvenile snapper (collected from the waters of American Samoa; Supplemental Table S1) were analyzed for ^{14}C by extracting core material (first year of growth). The same micromilling machine was used in a manner similar to other

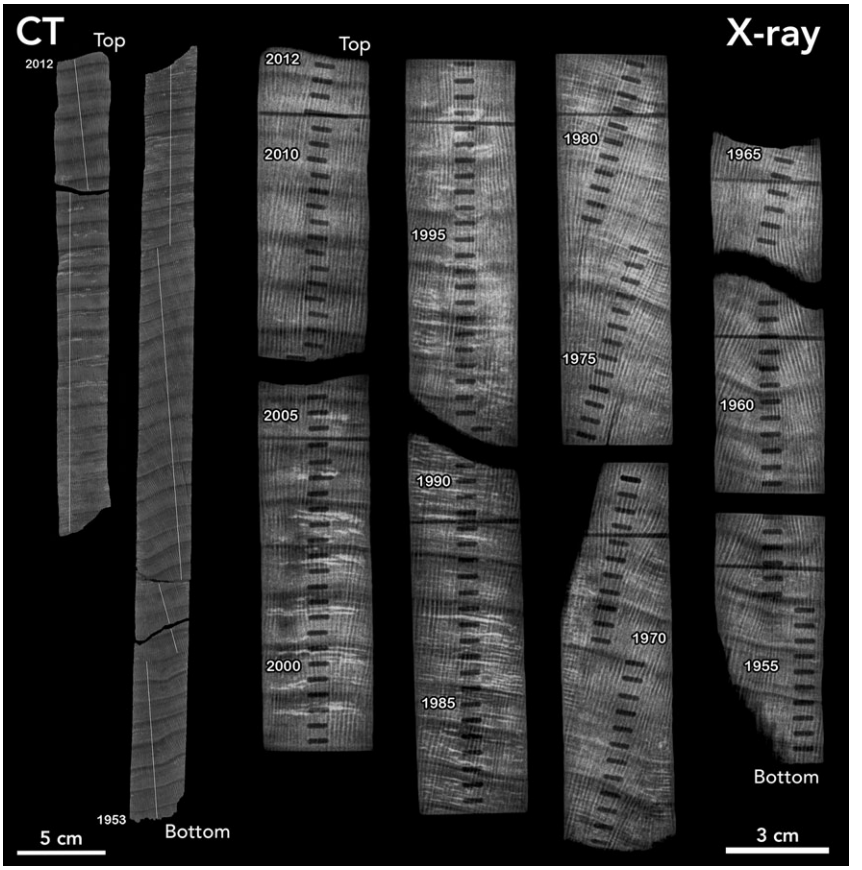

Figure 2 Pictured as a CT scan (left) and an X-ray (right) is the slabbed coral core extracted from a reef off Matautuloa Point on the southern side of Tutuila, American Samoa. The continuous CT scan and X-ray show a clear banding pattern across the core with the chronology labeled every 5 yr from the annual band counting (high- and low-density couplet) in the X-ray image. The record begins at the collection date in 2012 and clearly covers regularly spaced bands through to 1953 for a total of 59 yr of growth. The banding structure was consistent through time in each core image with a mean annual growth rate of ~1.2 cm·yr^{-1}. The serial sampling from the micromill is seen as regularly spaced parallel channels (4–5 mm long) in the X-ray that were cut into the coral. The horizontal marks toward the top of each core segment in the X-ray image are an artifact of the indexing slots used for LA-ICP-MS placement and the white lines on the CT image show the laser scan paths.

snapper studies of the Pacific Ocean (e.g., Andrews et al. 2020a). Because age is far less in question for these young fish and reliable growth zone counting methods were employed, the calculated dates of formation were used as reference ^{14}C measurements with other reference records (i.e., American Samoa coral ^{14}C record).

The extracted coral and otolith samples were submitted as carbonate to the National Ocean Sciences Accelerator Mass Spectrometry Facility (NOSAMS) at Woods Hole Oceanographic Institution in Woods Hole, Massachusetts. Radiocarbon measurements were reported by NOSAMS as Fraction Modern (F^{14}C), the measured deviation of the ^{14}C/^{12}C ratio from Modern. Modern is defined as 95% of the ^{14}C concentration of the National Bureau of

Standards Oxalic Acid I standard (SRM 4990B) normalized to $\delta^{13}C$ VPDB (–19‰) in 1950 AD (VPDB = Vienna Pee Dee Belemnite geological standard; Coplen 1996). Radiocarbon results were corrected for isotopic fractionation using $\delta^{13}C$ measured concurrently during AMS analysis and are reported here as date corrected $\Delta^{14}C$ (Reimer et al. 2004). Stable isotope $\delta^{13}C$ measurements by a stable isotope mass spectrometer were made on a CO_2 split taken from the CO_2 generated through acid hydrolysis.

Several time-series analyses were performed on the coral core geochemistry data in order to evaluate the strength of the annual signal and its application to independently verify the chronology. The elemental ratios (Sr/Ca and Ba/Ca) from the two core tracks had mean depth spacing of 80 ± 57 μm (±1 SD) and a mean deviation (chronology) spacing of 2.6 ± 0.3 d (±1 SD). For each elemental ratio, the tracks were combined, sorted, and then interpolated to a uniform interval (time: 3-d; depth: 90 μm). Power spectral density (PSD) estimates were computed for the interpolated records using Welch's method with a 1024-point Hamming window (3072 d) with 50% overlap. The $\delta^{13}C$ measurements had a mean chronological spacing of 127 ± 30 d (±1 SD), with a minimum of 68 d and maximum of 282 d. This record was interpolated to a uniform 80-d interval and then a PSD was computed using a 64-point Hamming window (5120 d) with 50% overlap. Given the error associated with the core chronology, an expected range of ± 100 d around the annual period (366 d) was used to identify focal energy in the annual signal.

Sea-surface temperature (SST) was obtained from the National Oceanographic Atmospheric Administration's (NOAA) 1/4° daily Optimum Interpolation gridded SST v2.1 (Huang et al. 2020) for available years starting in 1982. The gridded SST was interpolated (two-dimensional linear) to the core location to obtain an SST time-series record.

RESULTS AND DISCUSSION

Coral Chronology

Dating of the American Samoa coral core with density band counting—assuming one year is represented by one high-low density band pair (Lough and Barnes 1990)—yielded 59 yr of growth that spanned the time of collection in 2012 to 1953 (Figure 2). The banding pattern observed in the coral CT and X-ray images was well-defined and uncomplicated leading to calculated mean growth rates of 1.12 ± 0.13 cm·yr^{-1} and 1.20 ± 0.02 cm·yr^{-1}, respectively. These results were consistent with other Pacific coral (*Porites* spp.) records with annual growth rates of ~1–1.5 cm·yr^{-1} (e.g., Guilderson et al. 2000; Prouty et al. 2010, 2014). To confirm these observations, an annual growth rate was calculated from the temporal coral geochemistry cycles within the error associated with the core band chronology. This spectral analysis captured strong annual periodicities from the Sr/Ca and Ba/Ca ratios, as well as $\delta^{13}C$ data (Figure 3A, B, and C), that can be attributed to seasonal fluctuations in SST (e.g., Delong et al. 2007) and metabolic rates (e.g., Swart 1983). Initial peak counting of the inferred annual geochemical signals underestimated the chronology by up to 4 yr; however, inclusion of additional smaller inflexions (changes in curvature) in the Sr/Ca data, visible across 2-yr periods, led to corroboration of the annual band counting to a lifespan of 58–59 yr (Figure 4). These muted Sr/Ca levels for some parts of the coral core may be attributed to minor annual temperature changes—the annual SST range for the Samoan Archipelago is small, ~2–3ºC on average (~27–30ºC; Brainard et al. 2008; Pirhalla et al. 2011), as reflected in a Sr/Ca annual range of less than 0.5 mmol·mol^{-1} (<3ºC; Supplemental Figure S2). The annual SST variability is likely lower at the collection depth

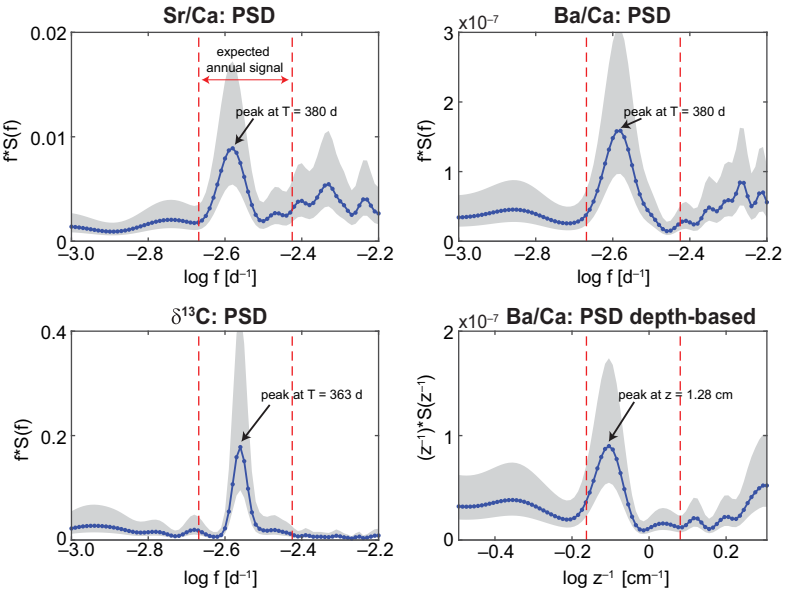

Figure 3 Power Spectral Density (PSD), $f^*S(f)$, estimates for (A) strontium:calcium (Sr/Ca) ratios, (B) barium:calcium (Ba/Ca) ratios, (C) stable carbon isotopes ($\delta^{13}C$), and (D) depth-based PSD ($z^{-1}*S(z^{-1})$) for the Ba/Ca ratios. For (A–C), the x-axis is $\log_{10}$ frequency (f) in cycles per day, and for (D) the x-axis is $\log_{10}$ cycles per cm. The red dashed lines indicate the frequency window considered for the annual signal (period range of 366 ± 100 d). The gray shading indicates the 95% confidence intervals.

of 10 m and on the southern side of Tutuila, in general, where waters were described as more mixed and less stratified than the northern side of the island (Brainard et al. 2008). As a result, the Sr/Ca-SST relationship may be weaker when the temperature range is narrow, similar to what was observed in Guam where the average annual SST range was <1°C (McCutcheon et al. 2015).

To further evaluate the relationship between the seasonal SST and these ratios, the magnitude-squared coherence (Cxy) was computed for the records cross-spectra. The coherence of annual periodicity was robust between SST and Ba/Ca ($Cxy = 0.45$, in phase) and moderate between SST and Sr/Ca ($Cxy = 0.21$, 180° out of phase). Therefore, the PSD was computed for the depth-based Ba/Ca record to independently estimate a growth rate. A conversion of 3.12×10^{-3} cm·d^{-1} was used to set the corresponding annual signal range for the depth-based PSD. Use of core depth instead of band counting indicated the annual Ba/Ca variance could be used to determine a growth rate of 1.28 ± 0.12 cm (Figure 3D), similar to the linear extension rates calculated from the CT and X-ray analyses (Prouty and Andrews 2020).

One of the most prominent features of the Sr/Ca time series from the American Samoa coral core is a shift in temperature between 1998 and 1999 with an elevated seasonal ^{14}C response. During this period, Sr/Ca ratios decreased from 9.79 to 9.12 mmol·mol^{-1} in less than 1 yr, indicating an SST increase of 3.5°C (Sr/Ca-SST calibration from 30-d average of interpolated SST data near Fatu Rock, Tutuila (OISST v2.1; Huang et al. 2020)). The calibration ($y = -5.2067x + 76.516$; $r = 0.732$) was applied down core for the Sr/Ca-derived SST record (Supplemental Figure S2). This increase in temperature appears robust because

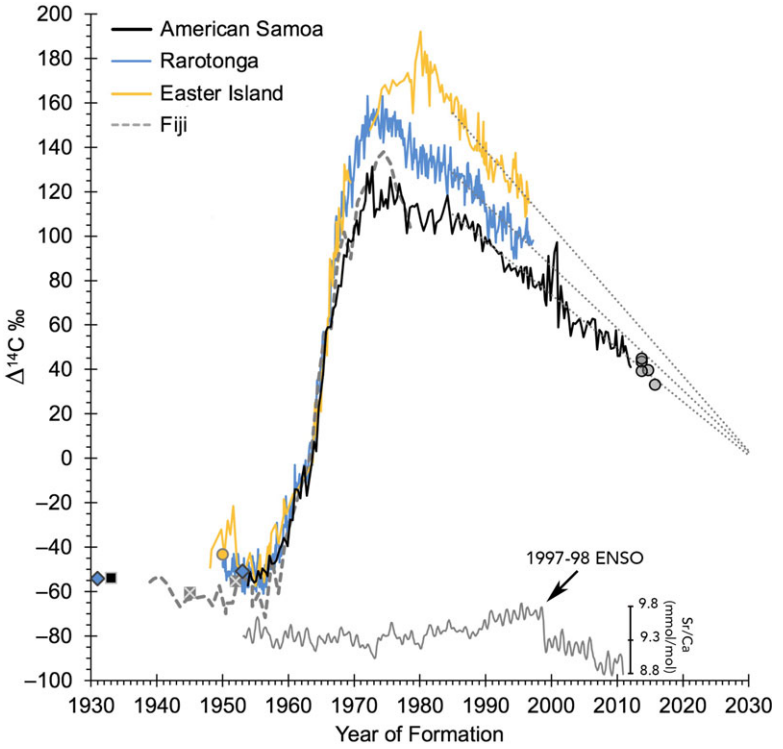

Figure 4 Plot of the ^{14}C record from American Samoa (1953–2012) with other regional coral records from the South Pacific Gyre (Fiji, Rarotonga and Easter Island; Toggweiler et al. 1991; Guilderson et al. 2000; Biddulph et al. 2006). The density band counting performed on the American Samoa coral was corroborated with annual strontium:calcium (Sr/Ca) peaks (8.8–9.8 mmol·mol^{-1}) that can be attributed to annual SST changes (range of ~27–30ºC). The ^{14}C levels associated with a recovery from the 1997–1998 ENSO event function as a regional marker that can be timed to ocean climate patterns. Post-peak ^{14}C levels for each coral record exhibit a monotonic decline after 1985 that appear to converge near 2030 (Sen's slope: American Samoa = –2.42, Rarotonga = –2.77, and Easter Island = –3.42 ‰·yr^{-1}). Fish otolith ^{14}C measurements (open grey circles in 2013–2015) follow the declining trend exhibited by the American Samoa coral record (Supplementary Table 1). Prebomb ^{14}C levels recorded in shell and coral fragments among locations were consistent with each regional coral record (black square = American Samoa, grey X = Fiji, blue diamond = Rarotonga, and yellow circle = Easter Island; Petchey et al. 2008).

the observed Sr/Ca decrease was detected in two separate LA-ICP-MS tracks, this period of coral growth was intact with no breaks in skeletal structure, and the OISST v2.1 data recorded a concomitant SST increase of 3.1ºC for the region (mid-1998 and early-1999). Within a few months of this well-documented warming event (1997–98 El Niño), there is a significant increase in $\Delta^{14}C$ to 91.0‰ in mid-1999 followed by a strong oscillation of ~30–40‰ in year 2000 and a $\Delta^{14}C$ maximum of 97.1‰, yielding a positive deviation of ~25‰ from a mean post-peak decline $\Delta^{14}C$ value of 71.6 ‰ (Figure 4). The implications of this shift are discussed below.

Climate Variability and ^{14}C

The timing of the events described above indicates the distinct changes in $\Delta^{14}C$ may be in response to the termination of the 1997–98 El Niño event—a recovery to La Niña conditions that would facilitate warming in the Samoan Archipelago (Pirhalla et al. 2011). This response is defined as a shift of the South Pacific Convergence Zone (SPCZ) toward the southwest, away from its average position crossing the Samoan Archipelago (175°W and 15–20°S; Gouriou and Delcriox 2002), leading to a decreased influence from higher salinity SEC waters (Linsley et al 2006), which would be expected to increase ^{14}C levels due a greater input from SPG waters and reduced influence from upwelled eastern boundary current waters from the Peru Current (Toggweiler et al. 1991). During the preceding El Niño event, a reversal of trade winds and deeper thermocline may have facilitated accumulation of ^{14}C-enriched surface waters in the eastern Pacific (Guilderson and Schrag 1998). These enriched ^{14}C surface waters could have been transported westward in the SEC to the Samoan Archipelago as a surge 12 mo later, assuming current speeds between 25–30 $cm{\cdot}s^{-1}$ as measured in the region for the SEC during ENSO conditions (Kendall et al. 2011). It is also important to note that Tutuila is in a unique location, situated at an average position for the SPCZ and a salinity front—shown to exhibit both short and long term atmospheric and ocean climate changes (Lindsley et al. 2006, Tangri et al. 2018)—that may complicate interpretation of annual ^{14}C cycles, including an out-of-phase annual ^{14}C cycle relative to SST observed for Rarotonga through the 1980s and 1990s (Guilderson et al. 2000). Weakening and strengthening of the SEC according to ENSO events, coupled with seasonal changes in SST and local upwelling, may be the basis for mixed ENSO responses in this region. It is also important to consider that differences in ^{14}C levels for tropical and subtropical waters are decreasing as post-peak levels in each region converge over time in response to the loss of bomb-produced ^{14}C to deep water and as the ocean becomes a net ^{14}C source to the atmosphere (Figure 4)—this crossover between ocean and atmosphere occurred near the year 2000 for the North Pacific Gyre (NPG) (Andrews et al. 2016c) and was shown as a 10-yr period of coincidence before overtaking atmospheric levels in 2010 for the Coral Sea (Wu et al. 2021). Hence, contrasting ^{14}C levels for waters advected from western equatorial sources relative to SPG sources should have less contrast over time.

The ^{14}C measurements from the American Samoa coral core provide a time series that is consistent with other regional records with some notable differences across the SPG (Figure 4). The ^{14}C levels during the pre-bomb period (1953–1956) were depleted with a mean of $\Delta^{14}C = -53.4 \pm 2.6‰$ ($n = 10$), consistent with a shell collected in 1933 at American Samoa ($\Delta^{14}C = -53.7‰$; Petchey et al. 2008). Pre-bomb levels were similar for the same period at Rarotonga ($\Delta^{14}C = -53.4 \pm 4.4‰$, $n = 71$; Guilderson et al. 2000), which was also consistent with shell and coral collected in 1931 and 1953 ($\Delta^{14}C = -54.2$ and $-50.9‰$ respectively; Petchey et al. 2008) and the extended mean of $\Delta^{14}C = -56.1 \pm 4.5‰$ ($n = 124$, 1950–1956; Guilderson et al. 2000). Pre-bomb $\Delta^{14}C$ values were elevated at Easter Island for the same 1953–1956 period ($\Delta^{14}C = -49.2 \pm 5.7‰$, $n = 10$), likely due to pooling effects of gyre waters, and while the sample size was smaller, pre-bomb $\Delta^{14}C$ Fiji values were lower ($\Delta^{14}C = -65.0 \pm 6.1‰$ $n = 3$) and consistent with coral and shell sample collected in 1945 and 1952, respectively ($\Delta^{14}C = -55.4$ and $-60.5‰$; Petchey et al. 2008). In contrast, Easter Island $\Delta^{14}C$ levels from 1949 to 1951 were elevated relative to other pre-bomb measurements (approaching $-20‰$ in 1951; Biddulph et al. 2006). The Easter Island ^{14}C-enrichment reflects its location near the SPG center where local convergence of

surface waters is less influenced by upwelled ^{14}C-depleted waters on the gyre margins (Broecker and Peng 1982). A similar observation was made at Fanning Island in the Central Equatorial Pacific (3.87°N, 159.32°W), but the timing and duration (1947–1956) of the enrichment was different and attributed to a long-term shift in the Pacific Decadal Oscillation (PDO; Grottoli et al. 2003). The offset observed for the Easter Island ^{14}C record may be more specifically linked to a strong Southern Oscillation recorded for 1949–1951 (Trenberth 1984; Keppene and Ghil 1992; Commonwealth of Australia 2021). This observation is further supported by an elevated ^{14}C measurement from an Easter Island shell collected in 1950 ($\Delta^{14}C = -43.1‰$; Petchey et al. 2008). This event is also correlated with SST data from coral $\delta^{18}O$ records at Rarotonga, Moorea and New Caledonia and may be related to a shift in the SPCZ where a similar response was not observed at Fiji (Linsley et al 2006). Unfortunately, the American Samoa coral core begins in 1953 and does not include this event.

For American Samoa, the bomb-produced ^{14}C rise began in 1957 and increased steadily to a maximum in the early 1970s. This rise time is similar to most coral records across the tropical-subtropical South Pacific with American Samoa, Rarotonga, Easter Island, and Fiji rising at similar rates (15.0, 15.5, 15.5, and 15.9 ‰·yr^{-1}, respectively) through the decade of most rapid rise (1958–1968), although there is a departure in 1966 of the American Samoa record to an attenuated peak ($\Delta^{14}C = 131$ ‰ in 1972 *cf.* $\Delta^{14}C = 163$ ‰ in 1974 for Rarotonga). Peak values across the three selected locations in the SPG follow a pattern that is similar to observations in the NPG, where coral bomb ^{14}C records trend toward more elevated peak values as the location becomes more centrally located in gyre waters (e.g., Andrews et al. 2016a, 2016c, Guilderson et al. 2021). For example, Rarotonga is ~1300 km southeast of American Samoa and more closely situated within the SPG, thereby influenced by greater surface water residence times and exposure of the mixed layer for air-sea diffusion of $^{14}CO_2$. In comparison, the coral ^{14}C record from American Samoa was expected to be more depleted due to mixing of upwelled waters from the eastern equatorial Pacific transported via the SEC (Broecker and Peng 1982; Broecker et al. 1985). This pattern is similar to what was observed for the NPG from a Hawaii Island coral ^{14}C record located at the southern end of the Hawaiian Archipelago and at the northern edge of the North Equatorial Current (Andrews et al. 2016c; Gulderson et al. 2021). In contrast, the ^{14}C record from Easter Island, being centrally located in the SPG where downwelling dominates, is expected to be the most elevated due to the greatest residence time for the mixed layer, as confirmed by elevated DI^{14}C values measured in the region (Key et al. 2004). The overall progression from an attenuated bomb ^{14}C signal at American Samoa to successively greater peak values at Rarotonga and Easter Island are in agreement with the bi-modal distribution of ^{14}C across the tropical-subtropical Pacific Ocean and the SPG (Linick 1980; Key et al. 2004). This spatial pattern is consistent with surface ocean measurements from programs like WOCE and GEOSECS that demonstrated how the distribution of bomb radiocarbon in the surface ocean is highly latitude-dependent, with the greatest $\Delta^{14}C$ values centered at approximately 30°N and 30°S (Linick 1980; Broecker et al 1985; Nydal 2000). The delayed peak at Easter Island can be attributed to its location within the warm, nutrient-poor subtropical water of the anticyclonic SPG (Reid et al. 1978; Moraga et al. 1999). Nonetheless, the regional post-peak ^{14}C signal for each record follows an expected monotonic decline—a pattern that is punctuated with inflexions for some periods but overall continues to decrease over time—for which the decrease in coral ^{14}C values is a function of air-sea diffusion and regional oceanography.

Post-peak $\Delta^{14}C$ levels decline episodically from the mid-1970s to the mid-1980s for the records closer to equatorial waters (Fiji, Rarotonga, and American Samoa). After each peak there is a rapid ^{14}C decline of 30–34 ‰ in 3–6 yr to a more moderate decline for a period of ~10 yr beginning in the late-1970s and ending in the late-1980s. While there is no information after 1978 for Fiji, the record for Rarotonga declines at ~1.7‰ per year as American Samoa comes close to leveling off at ~0.3‰ per year, similar to observations made for corals in the North Pacific during the same period (Andrews et al. 2016c, Guilderson et al. 2021). This long-period event is well-correlated in time with shifts observed in sea level pressure as a strong PDO for the North Pacific (1976–1988; Trenberth and Hurrell 1994; DiLorenzo et al. 2008), which may be responsible for the effect noted above on the northern edge of the SPG as is reflected in the Rarotonga and American Samoa coral ^{14}C records. After this period, each ^{14}C record begins to follow what may be a path of convergence despite episodic events that shift ^{14}C levels for a few years, like the significant ^{14}C pulse in the American Samoa record associated with the 1997–98 ENSO event. Despite these long-term inflexions and subannual pulses, a nonparametric (Mann-Kendall test) assessment for a monotonic trend provided Sen's slopes for the declining trends of –3.42 ‰·yr^{-1} (Easter Island), –2.77 ‰·yr^{-1} (Rarotonga), and –2.42 ‰·yr^{-1} (American Samoa), all of which may converge near the year 2030 (Figure 4). This decline is expected from the dilution and continued entrainment of ^{14}C-depleted waters from the lower thermocline (Jenkins et al. 2010), but the trend should also begin to reach an asymptote for surface waters as bomb-produced ^{14}C is sequestered from the air-sea environments and the tropical and subtropical seas approach pre-bomb equilibrium levels near –50‰. The American Samoa record adds to the evidence that ^{14}C in the tropical-subtropical waters of the Pacific are beginning to merge in the post-peak period, which provides opportunities to determine the age of short-lived marine organisms that provide an archive of ^{14}C variability through time.

Bomb ^{14}C Dating

One of the widest applications of bomb-produced ^{14}C as a tool in age determination is with ^{14}C stored in the otoliths (ear stones) of fishes. Otoliths are composed of calcium carbonate (aragonite) which calcify from marine DIC (Campana 1999). This inert non-skeletal structure is often used to provide estimates of age for fishes from purported annual growth zone structure, usually seen as growth rings in otolith cross sections, that is based strictly on visual interpretation and requires some form of validation (Campana 2001). The bomb-produced ^{14}C rise period is typically used as a temporal reference in determining the validity of an age estimate by alignment of ^{14}C measurements within the first year of otolith growth to a regional bomb ^{14}C reference. Because hermatypic (reef building) coral also sequester DIC as its carbon source for calcification, both the otolith and coral ^{14}C measurements can be compared directly for temporal alignment, or in some cases misalignment for which ages were not accurate. An example of a subtropical Pacific age validation study using otoliths and coral was on Hawaiian pink snapper (*Pristipomoides filamentosus*)—the estimated lifespan was thought to be 5–18 yr, with drastically different growth parameters, but was actually more than 40 yr based on bomb ^{14}C dating (Andrews et al. 2012). This is just one of many age validation studies throughout tropical-subtropical Pacific that have utilized the ^{14}C rise period as a time-specific marker with results that have provided age-validated life history characteristics that are essential in fisheries science (e.g., Kalish 1993; Andrews et al. 2011, 2015, 2016b, 2019a, 2020a).

The apparent convergence of coral ^{14}C records across the SPG provides an indication that more recently collected fish can be aged using the post-peak ^{14}C decline. As was demonstrated in a fortuitous study of a grander blue marlin (*Makaira nigricans*; 1245 lbs., 565 kg) captured in Hawaii, broad-scale convergence of ^{14}C records within the tropical-subtropical Pacific led to ^{14}C decline limits through time and a reliable age estimate of ~20 yr (Andrews et al. 2018). An apparent misalignment in time for measured otolith ^{14}C values from the coral ^{14}C decline can in some cases be explained by oceanography and early life history, as was attributed to a consistent offset of Pacific bluefin tuna (*Thunnus orientalis*) birth years (Ishihara et al. 2017)—these values were within the constraints of the collective coral ^{14}C records of the North Pacific and provided strong support for the age reading protocol to ~30 yr. In addition, an age reading protocol was refined based on a wide offset of otolith ^{14}C values from the regional decline reference and resulted in validated life history characteristics for a deep-water snapper that were drastically different from an initial otolith age reading interpretation (Andrews and Scofield 2021). In each case, the circumstances are specific to the early life history of the species and regional oceanography but the differences in ^{14}C levels for the tropical-subtropical Pacific across time and space are now reduced and appear to be converging. For the SPG, a set of otoliths from snapper collected from the Samoan Archipelago show evidence of a continued decline (Supplementary Table 1; Figure 4). These juvenile fish confirm that the validity of age estimates for adults of these species—collected from American Samoa and other parts of the archipelago—can be tested using the ^{14}C decline and further demonstrates that constraints can be placed on age for specimens across the SPG (e.g., a measurement of 60‰ is limited to birth years of ~2006–2013). While this level of precision is not optimal if one fish were aged in this manner (potential age range of ~7–14 yr), a proper age validation study must include numerous individuals that have been estimated for age using a consistent manner of growth zone counting (a well-defined age reading protocol) for specimens that cover the full lifespan. An example is from an age validation study of tuna from the Gulf of Mexico where numerous fish were aged with a well-defined protocol leading to a series of birth years that were in alignment with the coral ^{14}C record —these species can live 2–3 times longer than previously estimated (Andrews et al. 2020b). Furthermore, this declining ^{14}C relationship should be supported with measurements from juvenile fish (known dates of formation) that cover the adult birth year timespan. For example, if a species is estimated to live 20 yr and adults of all sizes are available from a collection year of 2020, then use of juveniles (e.g., age-0 fish) collected across the span of calculated adult birth years (2000 to 2020) can provide direct evidence that adult otolith cores (the juvenile portion of the otolith) will align with the ^{14}C reference if the age reading protocol is accurate. Alternatively, a full study can be facilitated with limited juvenile collections or otolith edge material of young fish that cover a portion of the decline period, with the assumption that the trend of otolith ^{14}C alignment continues in unison with the coral ^{14}C reference (i.e., Andrews 2020; Barnett et al. 2018; Andrews et al. 2020b, Andrews and Scofield 2021). Use of the post-peak bomb ^{14}C decline has also evolved with a novel line of research that uses core material of fish eye lenses to validate age (Patterson et al. 2020) and in the use of new technology (laser ablation accelerator mass spectrometry) to trace continuous bomb ^{14}C signals within an otolith (Andrews et al. 2019b).

CONCLUSION

The bomb ^{14}C record from a coral core at American Samoa provides the longest chronology for the SPG by extending the record from the pre-bomb period to 2012. A comparison with

other SPG coral records highlights the role of position within the gyre to influence the timing and magnitude of the bomb-produced ^{14}C peak and decline. The effects of the strong 1997–1998 ENSO event that were documented as a series of ^{14}C peaks that correspond to the intrusion of warmer waters during the following La Niña years highlight the oceanographic complexity of this location during large scale climate shifts, such as the broad scale drivers of the position of the SPCZ (e.g., Folland et al. 2002). The American Samoa ^{14}C chronology, when combined with other coral records, provides evidence for convergence of ^{14}C levels through the decline period in the SPG. This observation reinforces the perspective that recently collected fishes and other organisms of the tropical-subtropical marine mixed layer with conserved skeletal and non-skeletal structures can be aged using these records as a temporal reference and that bomb ^{14}C dating is no longer tied strictly to the initial ^{14}C rise period in the 1950s and 1960s as a temporal reference.

ACKNOWLEDGMENTS

We are very grateful to C. Young and D. Merritt for assistance with the core extraction (NOAA R/V *Hi'ialakai*), K. Rose (WHOI) and A. Cohen (WHOI) for CT analysis, C. Gallagher (UCSC) for LA-ICP-MS, the staff of VCA University Animal Hospital #468 in Honolulu for the coral X-ray (L. Iboshi, J.K.W. Ng, M. Malta, and C. Sharp), and W. Beck (U. Arizona) for providing an internal review and two anonymous reviewers for providing constructive input. Thanks to R. Humphreys (PIFSC), the Pacific Islands Fisheries Science Center, and the USGS Coastal and Marine Hazards and Resource Program's Coral Reef Project for project support. The coral core extraction was performed under the American Samoa Department of Marine and Wildlife Resources Scientific (Permit Series No. 2012-57), Fagatele Bay National Marine Sanctuary Research (Permit No. FBNMS-2011-002), National Park of American Samoa research (Permit No. NPSA-2012-SCI-0001), and Pacific Reefs National Wildlife Refuge Complex (Special Use Permit No. 12521-10001). Fish specimens were collected by the Pacific Islands Fisheries Science Center under Project SE-16-01 and data were accessed via the NOAA National Centers for Climate Information (https://www.ncdc.noaa.gov/paleo-search/study/27541). Any use of trade, product, or firm names is for descriptive purposes only and does not imply endorsement by the U.S. Government. Additional geochemical data to support this project can be found in Prouty and Andrews (2020) and in the Supplemental Material.

SUPPLEMENTARY MATERIAL

To view supplementary material for this article, please visit https://doi.org/10.1017/RDC.2021.51

REFERENCES

Andrews AH. 2020. Giant Trevally (*Caranx ignobilis*) of Hawaiian Islands can live 25 years. Marine and Freshwater Research 71:1367–1372. doi: 10.1071/MF19385

Andrews AH, Scofield TR. 2021. Early overcounting in otoliths: a case study of age and growth for gindai (*Pristipomoides zonatus*) using bomb ^{14}C dating. Fisheries and Aquatic Sciences 24:53–62. doi: 10.47853/FAS.2021.e6.

Andrews AH, Kalish JM, Newman SJ, Johnston JM. 2011. Bomb radiocarbon dating of three important reef-fish species using Indo-Pacific $\Delta^{14}C$ chronologies. Marine and Freshwater Research 62:1259–1269. doi: 10.1071/MF11080.

Andrews AH, DeMartini EE, Brodziak J, Nichols RS, Humphreys RL. 2012. A long-lived life history for a tropical, deepwater snapper (*Pristipomoides filamentosus*): bomb radiocarbon dating as extensions of daily increment analyses in otoliths. Canadian Journal of Fisheries Aquatic Sciences 69:1850–1869. doi: 10.1139/f2012-109.

Andrews AH, Choat JH, Hamilton RJ, DeMartini EE. 2015. Refined bomb radiocarbon dating of two iconic fishes of the Great Barrier Reef. Marine and Freshwater Research 66:305–316. doi: 10.1071/MF14086.

Andrews AH, Asami R, Iryu Y, Kobayashi DR, Camacho F. 2016a. Bomb-produced radiocarbon in the western tropical Pacific Ocean—Guam coral reveals operation-specific signals from the Pacific Proving Grounds. Journal of Geophysical Research Oceans 121:6351–6366. doi: 10.1002/2016JC012043.

Andrews, AH, DeMartini EE, Eble JA, Taylor BM, Lou DC, Humphreys RL. 2016b. A half-century lifespan for a keystone browser, the bluespine unicornfish (*Naso unicornis*), with a novel approach to bomb radiocarbon dating in the tropical North Pacific Ocean. Canadian Journal of Fisheries and Aquatic Sciences 73:1575–1586. doi: 10.1139/cjfas-2016-0019.

Andrews AH, Siciliano D, Potts DC, DeMartini EE, Covarrubias S. 2016c. Bomb radiocarbon and the Hawaiian Archipelago: coral, otoliths and seawater. Radiocarbon 58:531–548. doi: 10.1017/RDC.2016.32.

Andrews AH, Humphreys RL, Sampaga JD. 2018. Blue marlin (*Makaira nigricans*) longevity estimates confirmed with bomb radiocarbon dating. Canadian Journal of Fisheries and Aquatic Sciences 75:17–25. doi: 10.1139/cjfas-2017-0031.

Andrews AH, DeMartini EE, Brodziak J, Nichols RS, Humphreys RL. 2019a. Growth, longevity, and age at first maturity and sex change of Hawaiian grouper (*Hyporthodus quernus*)—input for management and conservation of a large, slow-growing grouper. Canadian Journal of Fisheries and Aquatic Sciences 76:1874–1884. doi: 10.1139/cjfas-2018-0170

Andrews AH, Yeman C, Welte C, Hattendorf B, Wacker L, Christl M. 2019b. Laser ablation accelerator mass spectrometry reveals complete bomb ^{14}C signal in an otolith with confirmation of 60-year longevity for red snapper (*Lutjanus campechanus*). Marine and Freshwater Research 70:1768–1780. doi: 10.1071/MF18265.

Andrews AH, Brodziak J, DeMartini EE, Cruz E. 2020a. Long-lived life history for onaga (*Etelis coruscans*) in the Hawaiian Islands. Marine and Freshwater Research 72. doi: 10.1071/MF20243.

Andrews AH, Pacicco A, Allman R, Falterman BJ, Lang ET, Golet W. 2020b. Validated longevity of yellowfin (*Thunnus albacares*) and bigeye (*Thunnus obesus*) tuna of the northwestern Atlantic Ocean. Canadian Journal of Fisheries and Aquatic Sciences 77: 637–643. doi: 10.1139/cjfas-2019-0328.

Barnett BK, Thornton L, Allman R, Chanton JP, Patterson WF. 2018. Linear decline in red snapper (*Lutjanus campechanus*) otolith $\Delta^{14}C$ extends the utility of bomb radiocarbon dating chronometer for fish age validation in the Northern Gulf of Mexico. ICES Journal of Marine Science 75:1664–1671. doi: 10.1093/icesjms/fsy043.

Biddulph DL, Beck JW, Burr GS, Donahue DJ. 2006. Two 60-year records of ^{129}I from coral skeletons in the South Pacific Ocean. Radioactivity in the Environment 8:592–598. doi: 10.1016/S1569-4860(05)08047-2.

Brainard R, Gove J, Helyer J, Kenyon J, Mancini F, Miller J, Myhre S, Nadon M, Rooney J, Schroder R, Smith E, Vargas-Angel B, Vogt S, Vroom P. 2008. Coral reef ecosystem monitoring report for American Samoa: 2002–2006. NOAA Special Report NMFS PIFSC. 472 p. + Appendices.

Broecker WS, Peng T-H. 1982. Tracers in the Sea. Columbia University: Lamont-Doherty Geological Observatory.

Broecker WS, Peng T-H, Ostlund G, Stuiver M. 1985. The distribution of bomb radiocarbon in the ocean. Journal of Geophysical Research Oceans 90:6953–6970. doi: 10.1029/JC090iC04p06953.

Campana SE. 1999. Chemistry and composition of otoliths: pathways, mechanisms and applications. Marine Ecological Progress Series 188:263–297.

Campana SE. 2001. Accuracy, precision and quality control in age determination, including a review of the use and abuse of age validation methods. Journal of Fish Biology 59:197–242. doi: 10.1111/J.1095-8649.2001.TB00127.X

Commonwealth of Australia. 2021. Southern Oscillation Index (SOI) since 1876. Bureau of Meteorology. URL: <http://www.bom.gov.au/climate/enso/soi/>. Accessed 2021 April 10.

Coplen TB. 1996. New guidelines for reporting stable hydrogen, carbon, and oxygen isotope-ratio data. Geochimica Cosmochimica Acta 60:3359–3360.

Crook ED, Cohen AL, Rebolledo-Vieyra M, Hernandez L, Paytan A. 2013. Reduced calcification and lack of acclimatization by coral colonies growing in areas of persistent natural acidification. Proceedings of the National Academy of Sciences 110(27):11044–11049. doi: 10.1073/pnas.1301589110.

Dana TF. 1971. On the reef corals of the world's most northern atoll (Kure: Hawaiian Archipelago). Pacific Science 25:80–87.

Darrenougue N, De Deckker P, Payri C, Eggins S, Fallon S. 2013. Growth and chronology of the rhodolith-forming, coralline red alga *Sporolithon durum*. Marine Ecological Progress Series 474:105–119.

DeLong KL, Quinn TM, Taylor FW. 2007, Reconstructing twentieth-century sea surface temperature variability in the southwest Pacific: A replication study using multiple coral Sr/Ca records from New Caledonia. Paleoceanography 22:PA4212. doi: 10.1029/2007PA001444.

Di Lorenzo E, Schneider N, Cobb KM, Franks PJS, Chhak K, Miller AJ, McWilliams JC, Bograd SJ, Arango H, Curchitser E, Powell TM, Riviére P. 2008. North Pacific Gyre oscillation links ocean climate and ecosystem change. Geophysical Research Letters 35:L08607.

Druffel ERM. 2002. Radiocarbon in corals: record of the carbon cycle, surface circulation and climate. Oceanography 15:122–127.

Fallon SJ, McCulloch MT, van Woesik R, Sinclair DJ. 1999. Corals at their latitudinal limits: laser ablation trace element systematics in *Porites* from Shirigai Bay, Japan. Earth and Planetary Science Letters 172:221–238.

Fallon SJ, Guilderson TP, Caldeira K. 2003. Carbon isotope constraints on vertical mixing and air-sea CO_2 exchange. Geophysical Research Letters 30:2289. doi: 10.1029/2003GL018049.

Folland CK, Renwick JA, Salinger MJ, Mullan AB. 2002. Relative influences of the Interdecadal Pacific Oscillation and ENSO on the South Pacific Convergence Zone. Geophysical Research Letters 29:21-1–21-4. doi: 10.1029/2001GL014201.

Gouriou Y, Delcriox T. 2002. Seasonal and ENSO variations of sea surface salinity and temperature in the South Pacific Convergence Zone during 1976–2000. Journal of Geophysical Research Oceans 107:SRF 12-1–12-14. doi: 10.1029/2001JC000830.

Grottoli AG, Eakin CM. 2007. A review of modern coral $\delta^{18}O$ and $\Delta^{14}C$ proxy records. Earth–Science Review 81:67–91. doi: 10.1016/j.earscirev.2006.10.001.

Grottoli AG, Gille ST, Druffel ERM, Dunbar RB. 2003. Decadal timescale shift in the ^{14}C record of a central equatorial Pacific coral. Radiocarbon 45:91–99. doi: 10.1017/S0033822200032422.

Grumet NS, Abram NJ, Beck JW, Dunbar RB, Gagan MK, Guilderson TP, Hantoro WS, Suwargadi BW. 2004. Coral radiocarbon records of Indian Ocean water mass mixing and wind-induced upwelling along the coast of Sumatra, Indonesia. Journal of Geophysical Research Oceans 109:C05003. doi: 10.1029/2003JC002087.

Guilderson TP, Schrag DP. 1998. Abrupt shift in subsurface temperatures in the tropical Pacific associated with changes in El Niño: Science 281:240–243. doi: 10.1126/science.281.5374.240.

Guilderson TP, Schrag DP, Goddard E, Kashgarian M, Wellington GM, Linsley BK. 2000. Southwest subtropical Pacific surface water radiocarbon in a high-resolution coral record. Radiocarbon 42:249–256.

Guilderson TP, Schrag DP, Druffel ERM, Reimer RW. 2021. Postbomb subtropical North Pacific surface water radiocarbon history. Journal of Geophysical Research Oceans 126: e2020JC016881. doi: 10.1029/2020JC016881.

Huang LC, Banzon VF, Freeman E, Graham G, Hankins B, Smith TM, Zhang HM. 2020. NOAA 0.25-degree Daily Optimum Interpolation Sea Surface Temperature (OISST) Version 2.1. 1987–2017. NOAA National Centers for Environmental Information. URL: <https://doi.org/10.25921/RE9P-PT57>. Accessed 2020 Oct 23.

Ishihara T, Abe O, Shimose T, Takeuchi Y, Aires-Da-Sliva A. 2017. Use of post-bomb radiocarbon dating to validate estimated ages of Pacific bluefin tuna, *Thunnus orientalis*, of the North Pacific Ocean. Fisheries Research 189:35–41. doi: 10.1016/j.fishres.2016.12.016.

Jenkins WJ, Elder KL, McNichol AP, von Reden K. 2010. The passage of the bomb radiocarbon pulse into the Pacific Ocean. Radiocarbon 52:1182–1190.

Jupiter S, Roff G, Marion G, Henderson M, Schrameyer V, McCulloch MT, Hoegh-Guldberg O. 2008. Linkages between coral assemblages and coral proxies of terrestrial exposure along a cross-shelf gradient on the southern great barrier reef. Coral Reefs 27:887–903.

Kalish JM. 1993. Pre- and post-bomb radiocarbon in fish otoliths. Earth and Planetary Science Letters 114:549–554. doi: 10.1016/0012-821X(93)90082-K.

Kendall MS, Poti M, Wynne T, Kinlan B, Bauer L. 2011. Ocean currents and larval transport among islands and shallow seamounts of the Samoan Archipelago and adjacent island nations. In: A biogeographic assessment of the Samoan Archipelago (Eds. Kendall M, Poti M) 3–26. NOAA Technical Memo NOS NCCOS 132, Silver Springs, MD.

Keppenne CL, Ghil M. 1992. Adaptive filtering and prediction of the southern oscillation index. Journal of Geophysical Research Atmospheres 97:20449–20454. doi: 10.1029/92JD02219.

Key RM, Kozyr A, Sabine CL, Lee K, Wanninkhof R, Bullister JL, Feely RA, Millero FJ, Mordy C, Peng T-H. 2004. A global ocean carbon climatology: results from Global Data Analysis Project (GLODAP). Global Geochemical Cycles 18:GB4031. doi: 10.1029/2004GB002247.

Kubota K, Shirai K, Murakami-Sugihara N, Seike K, Minami M, Nakamura T, Tanabe K. 2018. Bomb-^{14}C peak in the North Pacific recorded in long-lived bivalve shells (*Mercenaria stimpsoni*). Journal of Geophysical Research Oceans 123:2867–2881. doi: 10.1002/ 2017JC013678.

Linick TW. 1980. Bomb-produced carbon-14 in the surface water of the Pacific Ocean. Radiocarbon 22:599–606. doi: 10.1017/S0033822200009978.

Linsley BK, Kaplan A, Gouriou Y, Salinger J, deMenocal PB, Wellington GM, Howe SS. 2006. Tracking the extent of the South Pacific Convergence Zone since the early 1600s.

Geochemistry Geophysics Geosystems 7(4): Q05003. doi: 10.1029/2005GC001115.

Lough JM, Barnes DJ. 1990. Intra-annual timing of density band formation of Porites coral from the Great Barrier Reef. Journal of Experimental Marine Biology and Ecology 135:35–57. doi: 10.1016/0022-0981(90)90197-K.

McCutcheon AL, Raymundo LJ, Jenson JW, Prouty NG, Lander MA, Randall RH. 2015. Testing the strontium/calcium proxy for sea surface temperature reconstruction in the coral *Porites lutea* in Guam, Micronesia. Water and Environmental Research Institute of the Western Pacific, University of Guam. UOGML Technical Report 159, WERI Technical Report 152.

Mitsuguchi T, Hirota M, Paleo Labo AMS Dating Group, Yamazaki A, Watanabe T, Yamano H. 2016. Post-bomb coral $\Delta^{14}C$ record from Iki Island, Japan: possible evidence of oceanographic conditions on the northern East China Sea shelf. Geo-Mar Letters 36:371–377. doi: 10.1007/s00367-016-0456-4.

Moraga J. Valle-Levinson A, Olivares J. 1999. Hydrography and geostrophy around Easter Island. Deep Sea Research Part I 46:715–731.

Nydal R. 2000. Radiocarbon in the ocean. Radiocarbon 42:81–98.

Patterson WF, Barnett BK, TinHan TC, Lowerre-Barbieri SK. 2021. Eye lens $\Delta^{14}C$ validates otolith-derived age estimates of Gulf of Mexico reef fishes. Canadian Journal of Fisheries and Aquatic Sciences 78. doi: 10.1139/cjfas-2020-0237.

Petchey F, Anderson A, Zondervan A, Ulm S, Hogg A. 2008. New marine ΔR values for the South Pacific gyre region. Radiocarbon 50:373–397. doi: 10.1017/S0033822200053509.

Pirhalla D, Ransi V, Kendall MS, Fenner D. 2011. Oceanography of the Samoan Archipelago. In: Kendall M, Poti M, editors. A biogeographic assessment of the Samoan Archipelago. NOAA Techinal Memo NOS NCCOS 132, Silver Springs, MD. p. 3–26.

Prouty NG, Andrews AH 2020. Geochemistry time series and growth parameters from Tutuila, American Samoa coral record. U.S. Geological Survey Data Release. doi: 10.5066/P9DTWC3I.

Prouty NG, Field ME, Stock JD, Jupiter SD, McCulloch M. 2010. Coral Ba/Ca records of sediment input to the fringing reef of the southshore of Moloka´i, Hawai´i over the last several decades. Marine Pollution Bulletin 60:1822–1835. doi: 10.1016/j.marpolbul.2010.05.024.

Prouty NG, Storlazzi CD, McCutcheon AL, Jenson JW. 2014. Historic impact of watershed change and sedimentation to reefs along west-central Guam. Coral Reefs 33:733–749. doi: 10.1007/s00338-014-1166-x.

Ramos RD, Goodkin NF, Druffel ERM, Fan TY, Siringan FP. 2019. Interannual coral $\Delta^{14}C$ records of surface water exchange across the Luzon Strait. Journal of Geophysical Research Oceans 124:491–505. doi: 10.1029/2018JC014735.

Reid JL, Brinton E, Fleminger A, Venrick EL, McGowan JA. 1978. Ocean circulation and marine life. In: Charnock H, Deacon G, editors. Advances in Oceanography. Springer US. p. 65–130.

Reimer PJ, Brown TA, Reimer RW. 2004. Discussion: reporting and calibration of post-bomb ^{14}C data. Radiocarbon 46:1299–1304. doi: 10.1017/S0033822200033154.

Sinclair DJ, Kinsley LPJ, McCulloch MT. 1998. High resolution analysis of trace elements in corals by laser ablation ICP-MS. Geochimica et Cosmochimica Acta 62:1889–1901. doi: 10.1016/S0016-7037(98)00112-4.

Swart PK. 1983. Carbon and oxygen isotope fractionation in scleractinian corals: a review. Earth-Science Review 19:51–80.

Tangri N, Dunbar RB, Linsley BK, Mucciarone DM. 2018. ENSO's shrinking twentieth-century footprint revealed in a half-millennium coral core from the South Pacific Convergence Zone. Paleoceanography and Paleoclimatology 33:1136–1150. doi: 10.1029/2017PA003310.

Trenberth KE. 1984. Signal versus noise in the Southern Oscillation. Monthly Weather Review 112:326–32.

Trenberth KE, Hurrell JW. 1994. Decadal atmosphere-ocean variations in the Pacific. Climate Dynamics 9:303–319.

Toggweiler JR, Dixon K, Broecker WS. 1991. The Peru upwelling and the ventilation of the South Pacific thermocline. Journal of Geophysical Research Oceans 96:20467–20497. doi: 10.1029/91JC02063.

Wu Y, Fallon SJ, Cantin NE, Lough JM. 2021. Surface ocean radiocarbon from a Porites coral record in the Great Barrier Reef: 1945–2017. Radiocarbon. doi: 10.1017/RDC.2020.141.